applied sciences

MDPI

Article

Effect of Temperature and Pressure of Supercritical CO_2 on Dewatering, Shrinkage and Stresses of Eucalyptus Wood

Lin Yang [1,2]

[1] College of Furnishings and Industrial Design, Nanjing Forestry University, Nanjing 210037, China; yanglin@njfu.edu.cn

[2] Co-Innovation Center of Efficient Processing and Utilization of Forest Resources, Nanjing Forestry University, Nanjing 210037, China

Abstract: Supercritical CO_2 ($SuCO_2$) dewatering can mitigate capillary tension and reduce wood collapse. In this study, *Eucalyptus urophylla* × *E. grandis* specimens were dewatered by $SuCO_2$ at temperatures of 35, 40 and 55 °C, in pressures of 10 and 30 MPa, respectively, for 1h. Effects of temperature and pressure on dewatering rate, moisture content (MC) distribution and gradient, shrinkage and residual stress of wood after dewatering were investigated. The results indicate that the $SuCO_2$ dewatering rate is much faster than that of conventional kiln drying (CKD). The dewatering rate increases with increasing of temperature and pressure; however, pressure has a significant influence, especially for the high-temperature dewatering process; the MC distribution after 1h dewatering is uneven and MC gradients decrease with reducing of mean final MC of wood. MC gradients along radial direction are much smaller than that in tangential direction; collapse of wood significantly reduces after dewatering due to $SuCO_2$ decreasing the capillary tension, and residual stress of wood during dewatering is mainly caused by pressure of $SuCO_2$, which decreases with increasing temperature. $SuCO_2$ dewatering has great potential advantages in water-removal of wood prone to collapse or deformation.

Keywords: spercritical CO_2 dewatering; *Eucalyptus urophylla* × *E. grandis*; dewatering rate; moisture content distribution; shrinkage; residual stress

Citation: Yang, L. Effect of Temperature and Pressure of Supercritical CO_2 on Dewatering, Shrinkage and Stresses of Eucalyptus Wood. *Appl. Sci.* **2021**, *11*, 8730. https://doi.org/10.3390/app11188730

Academic Editors: Manuela Romagnoli, Vladimir Gryc and Federica Antonelli

Received: 24 August 2021
Accepted: 15 September 2021
Published: 18 September 2021

1. Introduction

Eucalyptus species are planted in large areas in China due to their short growth cycle and strong adaptability; they have become the most important plantation wood species, producing a wide range of renewable materials. Eucalyptus wood is mainly used as raw materials in pulp, paper and wood-based panels, such as plywood, fiber boards and particle boards [1,2]. Owing to having relatively good mechanical performance, recently there has been significant interest in increasing the amount of eucalyptus wood as a resource of higher value-added solid wood products [3–5]. However, eucalyptus woods are predominantly available from short rotation cycles, which are mainly composed of juvenile wood and small-diameter logs [6]. Thus, timbers and lumbers of eucalyptus species are inherently difficult to process due to their higher variability, high growing tensions and poor permeability. Particularly, some severe problems arise from the convective drying process, such as intense collapse, internal checks and high internal drying stresses, which are responsible for reducing the yield of timber manufacturing [3,7,8].

Wood physical and mechanical characteristics are intensively related to water [9–13]. Capillary tensions occurring in convective drying are responsible for collapse and internal checks of timbers from eucalyptus wood. Woods collapses when cell walls cannot resist the capillary tensions caused by free water rapid migrating from cell lumens [14–18]. Thus, solutions have been developed and tested to reduce or prevent severe collapse of eucalyptus wood [19–21]. One the one hand, drying wood at a low temperature as slowly as possible may relax internal tensions or promotes collapse recovery during convective drying. On the other hand, collapse and internal checks may be mitigated using special approaches, such as freeze-drying [22] or supercritical CO_2 ($SuCO_2$) dewatering [23], which may remove or eliminate the capillary tension during free water migration.

As is known, $SuCO_2$ fluid is an excellent transfer medium, which has wonderful properties, such as excellent solubility and heat transfer, non-toxicity, non-flammability, high recovery rate and strong process selectivity medium. As a green wood processing medium, $SuCO_2$ has been used successfully in wood industries, such as wood preservation, dying, extraction and thermochemical conversion due to its advantages of efficiency and environmental friendliness [24–26]. Conventional kiln drying (CKD) are widely used in the world, but resulting in excessive greenhouse gas and primary organic aerosols emissions for burning fossil fuel to obtain heat and steam [27], recently, dewatering wood using clean $SuCO_2$ fluid has been reported [28]. The water-removing mechanism of $SuCO_2$ fluid is attributed to the pressure difference between the CO_2 of the supercritical phase and the gas phase. Dewatering wood using $SuCO_2$ fluid differs from water evaporation in CKD of wood and may eliminate negative water tension maximally. Few collapses and cracks in wood were found after dewatering using $SuCO_2$ [29–31]. Thus, this dewatering method has great potential in such timbers as eucalyptus and poplar prone to collapse. There were some studies [32–34] investigating wood dewatering using $SuCO_2$, but few investigations were related to the refractory eucalyptus wood and the effect of $SuCO_2$ on shrinkage and drying stress [35,36].

In the present paper, *Eucalyptus urophylla* × *E. grandis* wood was dewatered using $SuCO_2$, at 35, 40 and 55 °C, in 10 and 30 MPa, respectively, for 1 h. The focus is, in particular, the systematical investigation into the interrelationship among temperature and pressure of $SuCO_2$ and dewatering rate, moisture distribution, drying stress and shrinkage during dewatering, will provide theoretical and practical support for improving the yield of eucalyptus timber manufacturing.

2. Materials and Methods

2.1. Materials

Green wood of *Eucalyptus urophylla* × *E. grandis* was supplied from Guangxi Provence, China. The trees were turned into logs and sealed with plastic films, and then were delivered to the wood Lab of Nanjing Forestry University. Thereafter, the logs were processed into boards with dimensions of 25 (R) × 30 (T) × 1000 (L) mm; after that, the boards were produced into end-matched specimens of 25 (R) × 30 (T) × 100 (L) mm for the subsequent $SuCO_2$ dewatering tests. The specimens were free of knots, and the initial moisture contents (MC) was about 110%.

2.2. Equipment

The main equipment is a $SuCO_2$ dewatering device (DY221-50-06, Huaan Supercritical Fluid Extraction Co., Ltd., Nantong, China). It includes (1) a CO_2 storage bottle; (2) a cooling circulating pump; (3) a big drying vessel (φ100, 5 L); (4) a small drying vessel (φ50, 2 L); and (5) and (6), two adsorption vessels (Figure 1). Liquid CO_2 was stored in the storage bottle (1) and then was delivered to the dewatering device by the circulating pump (2). The temperature of the drying vessels was controlled by a heated mantle. During dewatering process, the drying vessels could control pressure from 0.1 to 30 MPa, and temperature from 30 to 70 °C. Other equipment included an electric heating oven (DHG-905386-III, Shanghai Cimo Medical Instrument Co., Ltd., Shanghai, China), an electronic balance, 0.001 g (Sincere Dedication of Science and Technology Innovation Company, Shanghai, China) and a vernier caliper (CD-20CPX, Mitutoyo, Japan, 0–200 mm/0.01 mm).

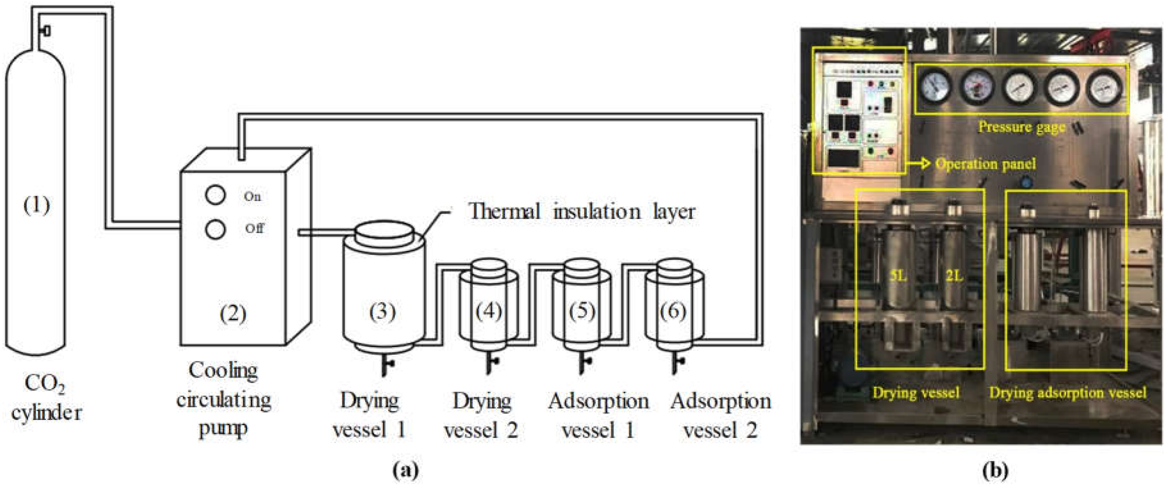

Figure 1. Supercritical CO_2 dewatering system. (**a**) Sketch map and (**b**) localized photo.

2.3. Dewatering Test

Each test had three end-matched specimens, whose mass and dimensions were measured prior to test. The specimens were inserted into the extraction vessel, and the dewatering tests were conducted according to the schedule in Table 1. For each run, the specimens were in full contact with $SuCO_2$ for 60 min after the temperature and pressure reached the setting values. Then, the pressure of CO_2 was decreased to atmospheric pressure (0.1 MPa) in 10 min due to escaping CO_2 gas; thereafter, the specimens were taken out from the drying vessel for a further cessation of CO_2 emission in room temperature. Finally, the specimens were used for the subsequent measurement of MC distribution, drying stress and shrinkage.

Table 1. Parameters of supercritical CO_2 dewatering process.

Process Parameter	Value
Supercritical temperature (°C)	35/40/55
Maximum pressure (MPa)	10/30
Minimum pressure (MPa)	0.1
Pressurization time (min)	10~30
Holding time (min)	60
Decompression time (min)	10
CO_2 emission time (min)	30

2.4. Moisture Content and Distribution Measurement

The initial MC prior to test and final MC after dewatering of wood were determined according to the China National Standard (GB/T 1931–2009). The MC samples were dried in an oven at (103 ± 2) °C until the absolute dry mass was obtained. MC was calculated according to Equation (1).

After dewatering, three 100-mm specimens were taken out from the vessels, and two 5-mm slices were cut from each specimen for MC and its distribution determination (Figure 2). Each slice was divided into 25 pieces via marking cross lines. Thereafter, the slice was cut into 25 wood blocks using a knife. The average MC and its distribution were determined using the exact MC of each block.

$$W = \frac{m_1 - m_0}{m_0} \times 100\% \tag{1}$$

where W is the MC, (%); m_1 is the initial mass, (g); and m_0 is the absolute dry mass, (g).

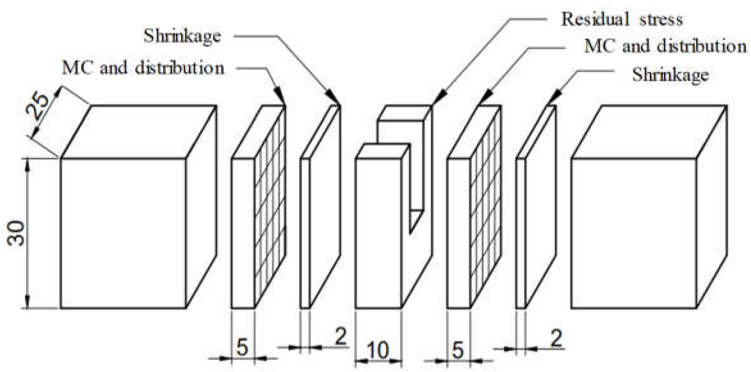

Figure 2. Sketch map of sample cutting.

2.5. Shrinkage Measurement

In this study, the shrinkage of wood after dewatering was determined based on the area in transverse section of the specimen [37]. As shown in Figure 2, two 2-mm slices were sawed from each specimen and then were scanned into images (300 dpi; Bit depth: 24) by a scanner (CanoScan LiDe 700F). Adobe Photoshop (Adobe Systems Inc., San Jose, CA, USA) was used to measure the pixel of the scanned images. The area of each slice was determined using the pixel of the scanned image. The shrinkage of the slices was calculated using Equation (2).

$$\beta = \frac{P_0 - P_1}{P_0} \times 100\% \tag{2}$$

where β is shrinkage, (%); P_0 is the pixel of the image of the initial slice sawing from two ends of specimen prior to dewatering, (px); and P_1 the pixel of the image of the slice sawing from the specimen after dewatering, (px).

2.6. Residual Stress Measurement

The residual stresses after dewatering of wood were measured using the prong test (GB/T 6491-2012). As shown in Figure 2, one 10-mm thickness slice was sawed from the middle of specimen and was employed for residual stress test. The slice was cut into a sample with a prong shape as shown in Figure 3. The initial thickness S of the specimen and the length L of prong edge were measured using a caliper (0–200 mm/0.01 mm). Thereafter, the slices were dried in an oven at (103 ± 2) °C for 3 h and then placed in ventilation place at room temperature for 24 h. After conditioning, the final dimension of S_1 was measured again using a caliper. The stress value Y is calculated using Equation (3):

$$Y = \frac{S - S_1}{2L} \times 100\% \tag{3}$$

where, Y is the residual stress value, (%); S is the initial thickness of the slices, (mm); S_1 the final thickness of the slices, (mm); and L is the prong length of slices, (mm).

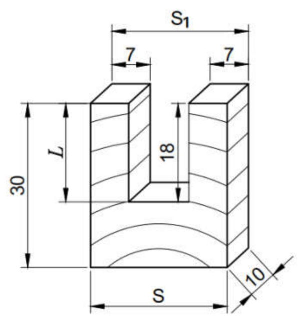

Figure 3. The prong processing and residual stress sample.

3. Results and Discussion

3.1. Dewatering Rate

Figure 4 shows the dewatering rate of *Eucalyptus urophylla* × *E. grandis* specimens after 1 h $SuCO_2$ dewatering. Moreover, the initial and final MCs of the specimens are also presented in the figure. The dewatering rate was compared with the drying rate of 5.5% per hour in CKD at 50 °C temperature and 84% relative humidity (RH) in previous study [35]. The dewatering rate using $SuCO_2$ is 5.2 to 11.7 times that of CKD. Fast removal of water in wood is important for timbers, which can prevent attacks of insects, shorten drying time and reducing storage cost of materials. Thus, $SuCO_2$ dewatering is beneficial for wood industry in these cases. For 10 MPa pressure, temperatures of 35, 40 and 50 °C dewatering, free water in wood was dewatered by 28.5, 32.6 and 34.8% per hour, respectively, and dewatering rate increased slowly with temperature rising. Similar results were also observed in dewatering at 30 MPa, 35 and 40 °C; however, in case of 55 °C, dewatering rate increased significantly. For the same temperature, dewatering rates increased more at higher pressure conditions. The average dewatering rate at 30 MPa is about 1.6 times to that at 10 MPa. All these findings suggest that dewatering using $SuCO_2$ is much faster than CKD; pressure significantly affects dewatering rate, and temperature has minor effect on dewatering rate at lower pressure. This finding is in agreement with previous report [28]. However, the effect of temperature on dewatering rate became obvious at higher pressure of 30 MPa in this study.

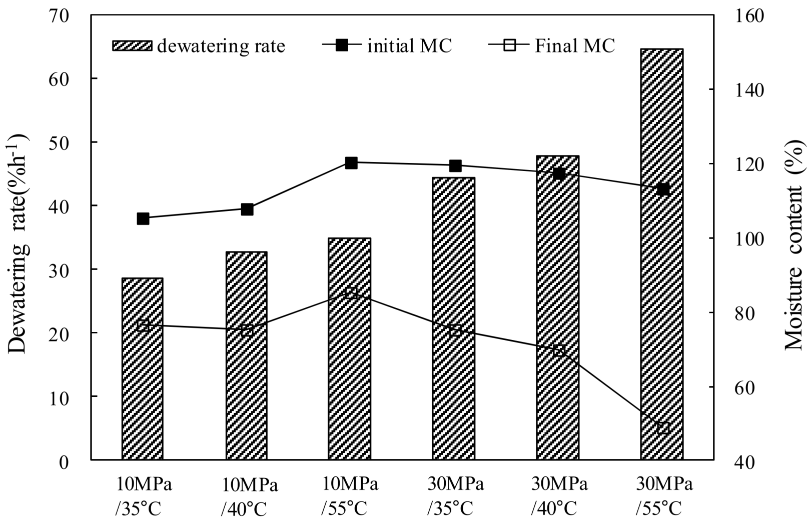

Figure 4. Effects of pressure and temperature on dewatering rate.

Dewatering rate relates to concentrations of dissolved CO_2 and wood permeability [38]. Higher pressure accelerates dissolving of CO_2, increasing the concentrations of CO_2 of the free water present in wood cell cavities [39]. During the decompression process, more CO_2 gas bubbles are generated in the free water of wood cell cavities, which expel water quickly from wood. Additionally, wood permeability affects CO_2 penetrating into wood and removal of water from wood. Wood permeability was improved by higher pressure of $SuCO_2$ [40], which benefits from penetration of CO_2 into wood and water removal from wood, thus resulting in higher dewatering rate at higher pressure of $SuCO_2$ dewatering.

3.2. Moisture Content Distribution

Figure 5 shows the 2D and 3D distributions of MC after 1 h $SuCO_2$ dewatering. The left and right part in Figure 5 indicates the status of MC after dewatering at 10 and 30 MPa, respectively. The mean final MCs and standard deviations of the 25 wood blocks in each dewatering test are shown in Figure 6. The standard deviations indicated as vertical bars present the MC gradients, which decline with decreasing of mean final MCs, showing that the larger MC gradients are present in the stage of higher mean final MC (10 MPa, 55 °C in

Figure 6). Similar phenomena are also observed in Figure 5, especially for the conditions of 30 MPa.

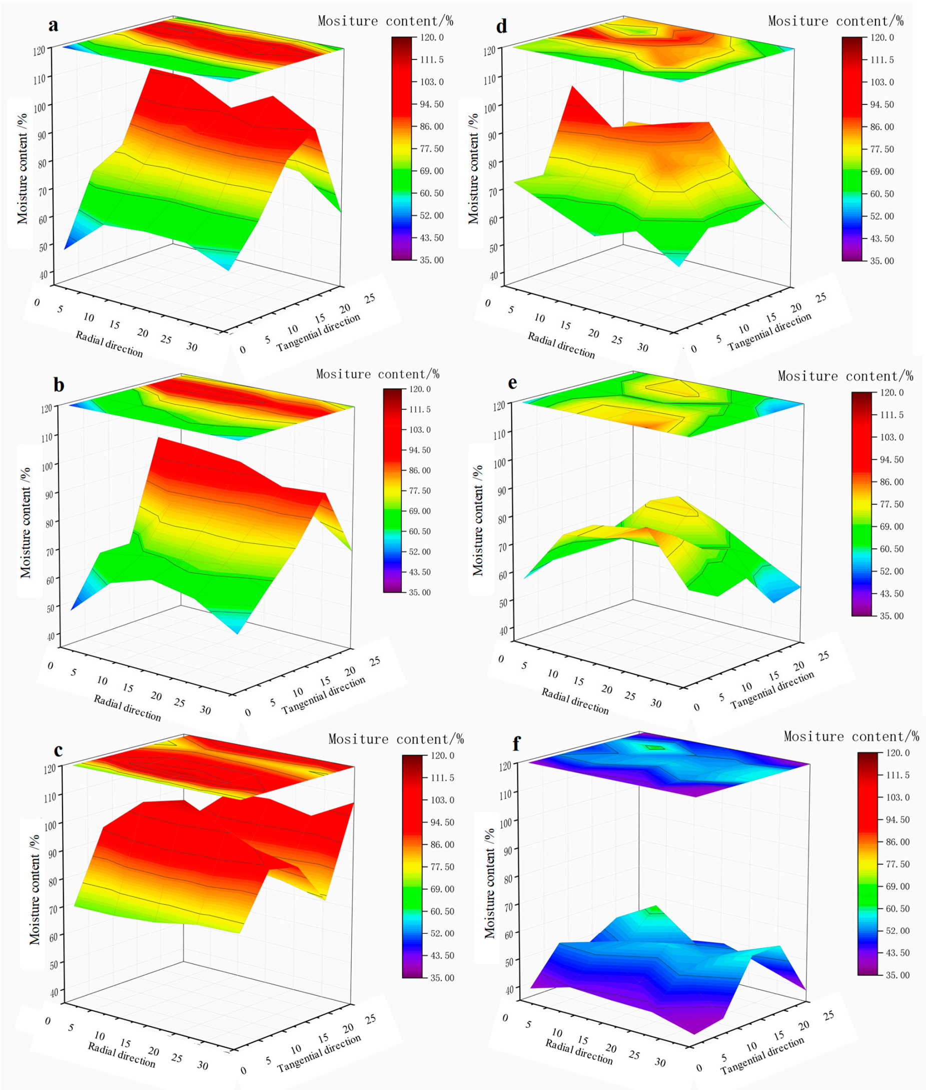

Figure 5. Distributions of wood final MC after 1 h $SuCO_2$ dewatering. (**a**): 10 MPa/35 °C, (**b**): 10 MPa/40 °C, (**c**): 10 MPa/55 °C; (**d**): 30 MPa/35 °C, (**e**): 30 MPa/40 °C, and (**f**): 30 MPa/55 °C.

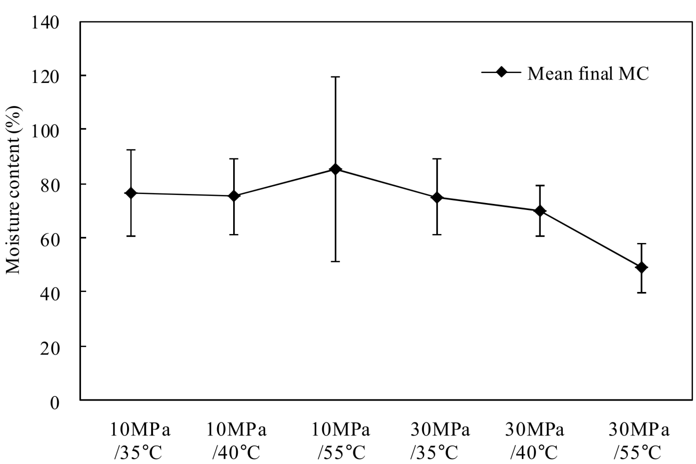

Figure 6. The mean MCs and standard deviations of six conditions after 1 h $SuCO_2$ dewatering.

The color gradients in Figure 5 show MC gradients of wood after dewatering. The color bands are the same or similar in radial direction compared with that in tangential direction, especially for the left part of 10 MPa pressure. This means that MC gradients along radial direction are much smaller than those in tangential direction. Moreover, MCs were higher in the central parts and lower in the surface parts of wood. MC gradients along tangential direction were greater, indicating water in wood was dewatered mainly in this direction. This result coincides with previous studies [32,36,41]. These phenomena could be explained by the bordered pits that control the water migration between connected cells. There are more bordered pits in radial cell walls of wood, resulting in further possible paths for water migration along tangential direction. During $SuCO_2$ dewatering, the dissolved CO_2 expands to bubbles of gas when releasing the pressure; free water is mainly expelled along tangential direction by bubbles of gas through the bordered pits connecting cell lumens towards the surfaces of wood.

3.3. Shrinkage

Figure 7 shows the effect of pressure and temperature on shrinkage of wood after 1 h $SuCO_2$ dewatering. Theoretically, wood shrinks as MC decreases to fiber-saturated point (FSP); however, shrinkages of wood were observed after $SuCO_2$ dewatering in each test when their MCs were over FSP (Figure 6). Collapse, an abnormal shrinkage, occurs when MC of wood is higher than FSP, which generally results in abnormal deformation. Severe collapses cause enormous loss of timber and high costs for industries. Therefore, the shrinkages in Figure 7 that occurred in each $SuCO_2$ dewatering indicate collapse of wood. However, the collapses of wood are only between 0.8% and 0.25%, which are much smaller than that of 2.8% in CKD and 3.6% in oven drying [35]. These results suggest that $SuCO_2$ dewatering may mitigate wood collapse and is in agreement with previous study [28]. Thus, $SuCO_2$ dewatering is an effective technology for improving timber drying quality. The less severe collapse is mainly attributed to the mechanism of $SuCO_2$ dewatering, which decreases capillary tension due to the fact free water in wood is expelled by CO_2 bubbles during decompression [32]. Additionally, collapse increases significantly with temperature at higher pressure dewatering.

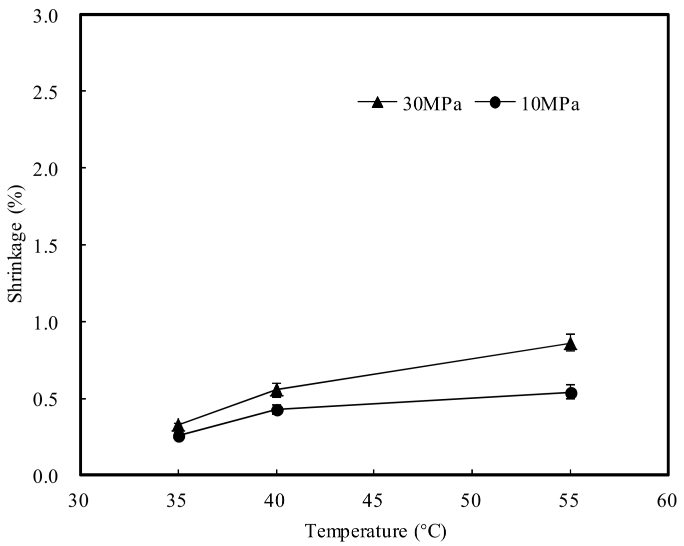

Figure 7. Effects of pressure and temperature on shrinkage.

3.4. Residual Stress

Figure 8 is the residual stress of wood after 1 h $SuCO_2$ dewatering test. The drying stresses at higher pressure were much greater than those at lower pressure and decreased with increasing temperature. These findings suggest that pressure mainly affects residual stress of wood in $SuCO_2$ dewatering process. Uneven shrinkage of wood causes stresses when MC of wood is lower than FSP with great gradients [42,43]. However, greater moisture content gradients also resulted in greater stresses during drying under high-pressure steam conditions when MC of wood is above FSP [44]. In this study, greater MC gradients in 10 MPa dewatering (Figures 5 and 6) resulted in smaller residual stresses, indicating residual stresses are caused mainly by pressure of supercritical CO_2 when MC of wood is above FSP.

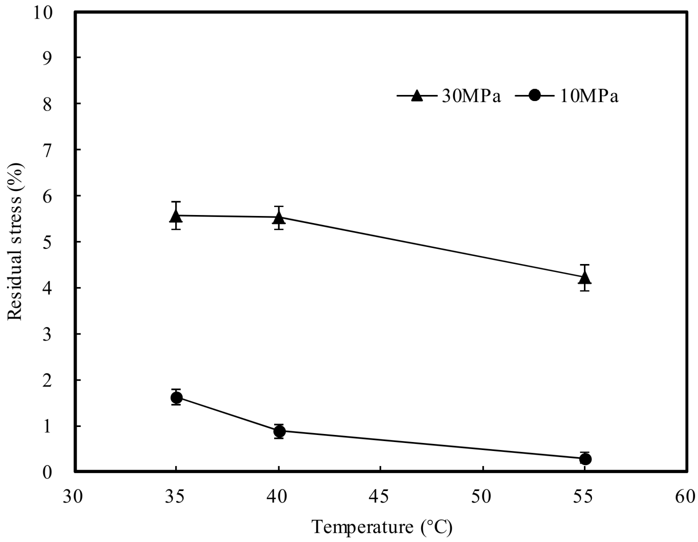

Figure 8. Effects of pressure and temperature on residual stress.

4. Conclusions

The results show that $SuCO_2$ dewatering is much faster than that of conventional kiln drying (CKD). Both temperature and pressure have an effect on dewatering rate during $SuCO_2$ dewatering, but pressure has a significant influence, especially on the high-temperature dewatering process. Moreover, the dewatering rate improves along with increasing temperature and pressure, while MC gradients of wood decline with decreasing wood mean final MC after 1 h dewatering. MC gradients along a radial direction are much smaller than that in a tangential direction and present uneven distribution in wood. The collapse of wood significantly reduces after dewatering due to capillary tension reduction caused by $SuCO_2$. Residual stresses of wood during dewatering are mainly caused by the pressure of $SuCO_2$, which decreases with increasing temperature. Owing to the fast dewatering rate and lowered collapse, $SuCO_2$ dewatering has great potential advantages in water removal of wood prone to collapse or deformation. Although temperature and pressure affect the characteristics of dewatering, shrinkage and stresses of wood, pressure has significant impacts. Parameters of pressure and temperature should be optimized to obtain high-quality eucalyptus timbers but reduce operating costs.

Funding: This research was funded by the National Natural Science Foundation of China (Grant No. 31870545) and Key Laboratory of Bio-based Material Science and Technology (Northeast Forestry University), Ministry of Education (SWZ-MS201903).

Institutional Review Board Statement: Not applicable.

Informed Consent Statement: Not applicable.

Data Availability Statement: Data sharing is not applicable to this article.

Conflicts of Interest: The authors declare no conflict of interest.

References

1. Yang, L.; Mao, H.Z.; Liu, H.H.; Wu, Z.H. Effect of freezing and compressing pre-treatment on collapse of *Eucalyptus Grandis* × *E. Urophylla* during drying. *J. For. Eng.* **2018**, *3*, 30–34. [CrossRef]

2. Zhou, Y.D.; Sun, F.; Lü, J.X.; Li, X.L. Veneer drying quality comparison of six eucalyptus species. *Sci. Silvae Sin.* **2014**, *50*, 104–108. [CrossRef]
3. Yang, L.; Liu, H.H. A review of Eucalyptus wood collapse and its control during drying. *BioResources* **2018**, *13*, 2171–2181. [CrossRef]
4. Chen, Y.S.; Zhu, J. Study on bending characteristics of fast growing eucalyptus bookcase shelves by using burgers model. *Wood Res.* **2019**, *64*, 137–144.
5. Teixeira, T.O.B.; Silva, M.L.; Jacovine, L.A.G.; Valverde, S.R.; Pires, V.A.V. A percepçao sobre o uso da madeira de eucalipto pelos fabricantes do polo moveleiro de Uba-MG The perception of manufacturers of the furniture center of Uba-MG about the use of eucalyptus wood. *Rev. Arvore* **2009**, *33*, 969–975. [CrossRef]
6. Washusen, R. *Processing Methods for Production of Solid Wood Products from Plantation-Grown Eucalyptus Species of Importance to Australia. (Project No. PNB291-1112A)*; Forest and Wood Products Australia: Melbourne, Australia, 2013.
7. Yin, Q.; Liu, H.H. Drying Stress and Strain of Wood: A Review. *Appl. Sci.* **2021**, *11*, 5023. [CrossRef]
8. Liu, H.H.; Zhang, J.W.; J, W.J.; Cai, Y.C. Characteristics of commercial-scale radio-frequency/ vacuum (RF/V) drying for hardwood Lumber. *Bioresources.* **2019**, *14*, 6923–6935. [CrossRef]
9. Cai, C.; Zhou, F.; Cai, J. Bound water content and pore size distribution of thermally modified wood studied by NMR. *Forests* **2020**, *11*, 1279. [CrossRef]
10. Li, R.; Fang, L.; Xu, W.; Xiong, X.; Wang, X. Effect of laser irradiation on the surface wettability of poplar wood. *Sci. Adv. Mater.* **2019**, *11*, 655–660. [CrossRef]
11. Hu, W.G.; Li, S.; Liu, Y. Vibrational characteristics of four wood species commonly used in wood products. *Bioresources.* **2021**, *16*, 7101–7111. [CrossRef]
12. Liu, X.Y.; Lv, M.Q.; Liu, M.; Lv, J.F. Repeated Humidity Cycling's Effect on Physical Properties of Three Kinds of Wood-based Panels. *Bioresources* **2019**, *14*, 9444–9453. [CrossRef]
13. Cai, C.Y.; Haapala, A.; Rahman, M.H.; Tiitta, M.; Tiitta, V.; Tomppo, L.; Lappalainen, R.; Heräjärvi, H. Effect of 2-year Natural Weathering on Chemical and Physical Properties of Thermally Modified *Picea abies*, *Pinus sylvestris* and *Fraxinus Excelsior*. *Can. J. For. Res.* **2020**, *50*, 1160–1171. [CrossRef]
14. Wu, Y.H.; Jia, R.; Ren, H.Q.; Zhou, Y.D.; Xing, X.T.; Wu, Z.K.; Wang, Y.R. Study on radial variation of main physical properties of imported *Pinus radiata* wood. *J. For. Eng.* **2019**, *4*, 48–53. [CrossRef]
15. Chafe, S.C. The distribution and interrelationship of collapse, volumetric shrinkage, moisture content and density in trees of *Eucalyptus Regnans* F. Muell. *Wood Sci. Technol.* **1985**, *19*, 329–345. [CrossRef]
16. Kauman, W.G. Cell collapse in wood—part I: Process variables and collapse recovery. *Holz. Roh. Werkst.* **1964**, *22*, 183–196. [CrossRef]
17. Perez-Pena, N.; Cloutier, A.; Segovia, F.; Salinas, C.; Sepulveda, V.; Salvo, L.; Elustondo, D.M.; Ananias, R.A. Hygromechanical strains during the drying of *Eucalyptus nitens* boards. *Maderas-Cienc. Tecnol.* **2016**, *18*, 235–244. [CrossRef]
18. Perez-Pena, N.; Elustondo, D.; Valenzuela, L.; Ananías, R.A. Variation of perpendicular compressive strength properties related to anatomical structure and density in *Eucalyptus nitens* Green Specimens. *BioResources* **2020**, *15*, 987–1000.
19. Kong, L.L.; Zhao, Z.J.; He, Z.B.; Yi, S.L. Development of schedule to steaming prior to drying and its effects on *Eucalyptus Grandis* × *E. Urophylla* wood. *Eur. J. Wood Wood Prod.* **2018**, *76*, 591–600. [CrossRef]
20. Peres, M.L.; Delucis, R.D.A.; Gatto, D.A.; Reltrame, R. Solid wood bending of *Eucalyptus grandis* wood plasticized by steam and boiling. *Ambient Constr.* **2015**, *15*, 169–177. [CrossRef]
21. Vermaas, H.F. Drying eucalypts for quality: Material characteristics, pre-drying treatments, drying methods, schedules and optimization of drying quality. *S. Afr. For. J.* **1995**, *174*, 41–49. [CrossRef]
22. Yang, L.; Ma, Q.Y.; Liu, H.H.; Liao, X.M.; Wu, Z.H. Freeze-drying properties of *Eucalyptus urophylla* × *E.grandis* wood. *J. For. Environ.* **2018**, *38*, 277–283. (In Chinese)
23. Gabitov, R.F.; Khairutdinov, V.F.; Gumerov, F.M.; Gabitov, F.R.; Zaripov, Z.I.; Gaifullina, R.; Farakhov, M.I. Drying and impregnation of wood with propiconazole using supercritical carbon dioxide. *Russ. J. Phys. Chem. B* **2017**, *11*, 1223–1230. [CrossRef]
24. Yu, X.R.; Liu, Y.; Luo, X.L.; Li, L.P.; Zhang, J.Y.; Zhao, P. Comparative analysis of volatile components extracted from the leaves of four Chinese fir clones. *J. For. Eng.* **2020**, *5*, 127–132. [CrossRef]
25. Ferrentino, G.; Morozova, K.; Mosibo, O.K.; Ramezani, M.; Scampicchio, M. Biorecovery of antioxidants from apple pomace by supercritical fluid extraction. *J. Clean. Prod.* **2018**, *186*, 253–261. [CrossRef]
26. Zhang, J.W.; Yang, L.; Liu, H.H. Green and efficient processing of wood with supercritica1 CO_2: A review. *Appl. Sci.* **2021**, *11*, 3929. [CrossRef]
27. Yao, Y.; Qin, H.S.; Fu, W.; Cui, C.; Liu, Y.B.; Gong, Y.L. Energy consumption analysis of drying of *Hevea brasiliensis* using solar energy-heat pump combined kiln. *J. For. Eng.* **2019**, *4*, 29–35. [CrossRef]
28. Franich, R.A.; Gallagher, S.; Kroese, H. Dewatering green sapwood using carbon dioxide cycled between supercritical fluid and gas phase. *J. Supercrit. Fluids* **2014**, *89*, 113–118. [CrossRef]
29. Dawson, B.S.W.; Pearson, H.; Kroese, H.W.; Sargent, R. Effect of specimen dimension and pre-heating temperature on supercritical CO_2 dewatering of radiata pine sapwood. *Holzforschung* **2015**, *69*, 421–430. [CrossRef]
30. Dawson, B.S.W.; Pearson, H. Effect of supercritical CO_2 dewatering followed by oven-drying of softwood and hardwood timbers. *Wood Sci. Technol.* **2017**, *51*, 771–784. [CrossRef]

31. Dawson, B.S.W.; Pearson, H.; Kimberley, M.O.; Davy, B.; Dickson, A.R. Effect of supercritical CO_2 treatment and kiln drying on collapse in *Eucalyptus nitens* wood. *Eur. J. Wood Wood Prod.* **2020**, *78*, 209–217. [CrossRef]
32. Newman, R.H.; Franich, R.A.; Meder, R.; Hill, S.J.; Kroese, H.; Sandquist, D.; Hindmarsh, J.; Schmid, M.W.; Fuchs, J.; Behr, V.C. Proton magnetic resonance imaging used to investigate dewatering of green sapwood by cycling carbon dioxide between supercritical fluid and gas phase. *J. Supercrit. Fluids* **2016**, *111*, 36–42. [CrossRef]
33. Meder, R.; Franich, R.A.; Callaghan, P.T.; Behr, V.C. A Comparative study of dewatering of pinus radiata sapwood using supercritical CO_2 and conventional forced air-drying via in situ magnetic resonance microimaging (MRI). *Holzforschung* **2015**, *69*, 1137–1142. [CrossRef]
34. Franich, R.A.; Meder, R.; Falge, M.; Fuchs, J.; Behr, V.C. Uncovering supercritical CO_2 wood dewatering via interleaved ^{1}H-imaging and ^{13}C-spectroscopy with real-time reconstruction. *J. Supercrit. Fluids* **2019**, *144*, 56–62. [CrossRef]
35. Zhang, J.W.; Liu, H.H.; Yang, H.; Yang, L. Drying characteristics of *Eucalyptus urophylla* $\times$ *E. grandis* with supercritical CO_2. *Materials* **2020**, *13*, 3989. [CrossRef]
36. Yang, L.; Liu, H.H. Effect of Supercritical CO_2 drying on moisture transfer and wood property of *Eucalyptus urophydis*. *Forests* **2020**, *11*, 1115. [CrossRef]
37. Yang, L.; Liu, H.H.; Cai, Y.C.; Wu, Z.H. A novel method of studying the collapsed cell of eucalyptus wood using X-ray CT scanning. *Dry. Technol.* **2019**, *37*, 1597–1604. [CrossRef]
38. Ramsey, E.; Sun, Q.B.; Zhang, Z.Q.; Zhang, C.M.; Gou, W. Mini-Review: Green sustainable processes using supercritical fluid carbon dioxide. *J. Environ. Sci.* **2009**, *21*, 720–726. [CrossRef]
39. Fernandes, J.; Kjellow, A.W.; Henriksen, O. Modeling and optimization of the supercritical wood impregnation process-focus on pressure and temperature. *J. Supercrit. Fluids* **2012**, *66*, 307–314. [CrossRef]
40. Hou, S.X.; Maitland, G.C.; Trusler, M. Measurement and modeling of the phase behavior of the (carbon dioxide + water) mixture at temperatures from 298.15 K to 448.15 K. *J. Supercrit. Fluids* **2013**, *73*, 87–96. [CrossRef]
41. Behr, V.C.; Hill, S.J.; Meder, R.; Sandquist, D.; Hindmarsh, J.P.; Franich, R.A.; Newman, R.H. Carbon-13 NMR Chemical-shift Imaging Study of dewatering of green sapwood by cycling carbon dioxide between the supercritical fluid and gas phases. *J. Supercrit. Fluids* **2014**, *95*, 35–540. [CrossRef]
42. Yue, K.; Song, X.L.; Cheng, X.C.; Lai, Y.J.; Jia, C.; Lu, W.D.; Liu, W.Q. Study on moisture stresses in Chinese fir glued laminated timber. *J. For. Eng.* **2019**, *4*, 35–40. [CrossRef]
43. Moutee, M.; Fortin, Y.; Fafard, M. A global rheological model of wood cantilever as applied to wood drying. *Wood Sci. Technol.* **2007**, *41*, 209–234. [CrossRef]
44. Cheng, W.L.; Liu, Y.X.; Morooka, T.; Norimoto, M. Characteristics of shrinkage stress of wood during drying under high temperature and high pressure steam conditions. *J. Beijing For. Univ.* **2005**, *27*, 101–106. [CrossRef]